PHYSICAL REVIEW B **72**, 081402(R) (2005)

# Phase determination in nuclear resonant scattering using a velocity drive as an interferometer and phase shifter

R. Callens,[1] C. L'abbé,[1] J. Meersschaut,[1] I. Serdons,[1] W. Sturhahn,[2] and T. S. Toellner[2]
[1]*Instituut voor Kern- en Stralingsfysica, K.U.Leuven, Celestijnenlaan 200D, B-3001 Leuven, Belgium*
[2]*Advanced Photon Source, Argonne National Laboratory, Argonne, Illinois 60439, USA*
(Received 12 April 2005; published 10 August 2005)

A scheme in which a velocity drive serves as an interferometer and phase shifter in nuclear resonant scattering experiments is presented, and a straightforward algorithm for phase determination is developed. The experimental feasibility of the concept is demonstrated for nuclear forward scattering by an $\alpha$-iron foil for different directions of the hyperfine field. It is also shown that the obtained phase information can be used for the reconstruction of the energy spectrum.

DOI: 10.1103/PhysRevB.72.081402 PACS number(s): 42.30.Rx, 42.25.Hz, 76.80.+y

Many characterization techniques in science are based on the scattering of radiation or particles. From fundamental quantum mechanics, we know that all information carriers can be regarded as waves, which can be described by a complex wave function. In most experiments, only the norm of this wave function is accessible via the square root of the measured intensity. The information about the phase of the wave function is typically lost. However, this information is crucial for the transformation to reciprocal space, i.e., the transformation between time and energy domain or between momentum transfer and real space. This is the so-called phase problem to which a solution was presented in 1948 by Gabor when he proposed holography.[1] He showed that phase information can be obtained by designing the experiment in such a way that interference occurs between the unknown object path and a well known reference path.

In this paper, we will focus on the phase determination of nuclear resonantly scattered synchrotron radiation. The nuclear resonant scattering technique is the time analog of Mössbauer spectroscopy and was developed about 20 years ago.[2] Since then, the brilliance of the synchrotron radiation beams has drastically increased and nuclear resonant scattering has become a powerful tool to study electric and magnetic properties in solids (for an overview see Refs. 3 and 4). Especially for the study of samples containing a small amount of the resonant Mössbauer isotope, e.g., samples embedded in a high pressure cell,[5–7] thin films,[8–11] or nanostructures,[12,13] the small beam size and the high directionality of the synchrotron beam are more advantageous than the highly divergent beam of a radioactive Mössbauer source. The difficulty for phase determination in nuclear resonant scattering experiments lies in the fact that the nuclear resonance energy is typically of the order of 10 keV, which corresponds to a wavelength of about 1 Å. For such short wavelengths, beam-splitting interferometers are difficult to implement. Although proven feasible,[14,15] one has to take care of the thermal and mechanical stability of the interferometer, which limits the sample space.

Here we propose an alternative approach. When the sample under investigation and a reference sample are placed one behind the other, several coherent paths are created [see Fig. 1(a)]. The unknown path is given by scattering by the sample under investigation, while the reference path is given by scattering by the reference sample. A third path describes the coupling of the samples by the radiation field. If the resonance energies in both samples differ substantially, this latter path can be neglected,[16–19] and an algorithm similar to the one described by Sturhahn[20] can be developed. By giving the reference sample a sufficiently high velocity, its resonance energy can be Doppler shifted to a region fulfilling this condition. Consequently, a reference sample mounted on a velocity drive that is placed in line with the sample under investigation [Fig. 1(b)], is equivalent to a setup with both samples placed in the spatially separated paths between the blades of a triple Laue interferometer. The main advantage of the setup with the velocity drive is that its simplicity allows for an easy extension to various sample environments and scattering geometries. For this rather simple experimental scheme, we developed an algorithm that gives direct access to the phase information.

The algorithm will be explained for a 100% linearly $\sigma$ polarized incident beam and a single-line reference sample, but it can easily be extended to other beam polarizations or other reference samples. After nuclear resonant scattering by a single-line reference sample with resonance frequency $\omega_r$, the wave field is still $\sigma$ polarized and can be written as

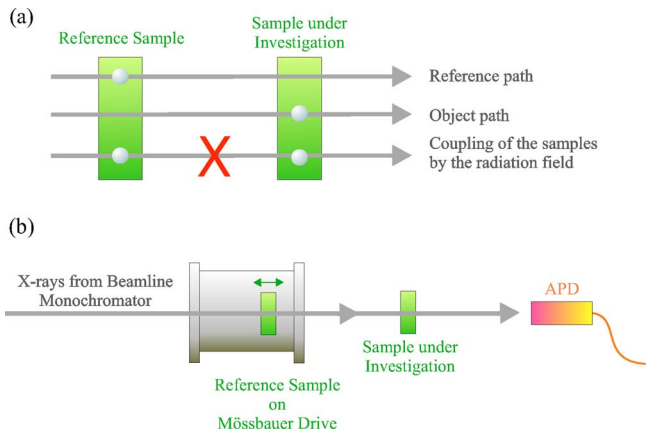


FIG. 1. (Color online) (a) Overview of the possible scattering paths. (b) Experimental scheme.

 

$$\vec{E}_r(t) = |E_r(t)|e^{-i\omega_r t}\vec{e}_\sigma. \quad (1)$$

If the reference sample is moving, its resonance frequency $\omega_r$ will be Doppler shifted by $\Delta = \omega_r v/c$, with $v$ the velocity of the sample projected on the photon direction and $c$ the speed of light. As a consequence, the wave field after forward scattering by the moving reference sample is given by

$$\vec{E}_r^{\Delta}(t) = |E_r(t)|e^{-i(\omega_r+\Delta)t}\vec{e}_\sigma = e^{-i\Delta t}\vec{E}_r(t). \quad (2)$$

From this equation it is clear that the velocity drive does not only serve as an interferometer, but that it can also be regarded as a phase shifter. Moreover, by varying the velocity of the reference sample, the phase of the reference wave field can be changed in a controlled way, which is required for the determination of the sign of the unknown phase.

For $t \neq 0$ and for velocities $v$ of the reference sample that are high enough so that the radiative coupling between both samples can be neglected, the wave field after both samples reduces to[21] $\vec{E}_r^{\Delta}(t) + \vec{E}_s(t)$, with $\vec{E}_s(t)$ the unknown wave field. This wave field generally has two polarization components and can be written as

$$\vec{E}_s(t) = |E_\sigma(t)|e^{i\varphi_\sigma(t)}\vec{e}_\sigma + |E_\pi(t)|e^{i\varphi_\pi(t)}\vec{e}_\pi. \quad (3)$$

The time evolution of the nuclear resonant scattered intensity is proportional to the square of the total wave field,

$$\begin{aligned} I(t,\Delta) &\sim |\vec{E}_r^{\Delta}(t) + \vec{E}_s(t)|^2 \\ &\sim |\vec{E}_r^{\Delta}(t)|^2 + |\vec{E}_s(t)|^2 \\ &\quad + 2|E_\sigma(t)||E_r(t)|\cos[\varphi_\sigma(t) + \omega_r t + \Delta t]. \end{aligned} \quad (4)$$

The intensity consists of two parts. The terms $|\vec{E}_r^{\Delta}(t)|^2 = |\vec{E}_r(t)|^2$ and $|\vec{E}_s(t)|^2$ describe the scattering by only the reference sample and only the sample under investigation, respectively. These contributions can be determined from two separate measurements where only one sample is placed in the beam. The last term of Eq. (4) describes the interference between the $\sigma$ component of the unknown wave field and the reference wave field. This term is proportional to the projection of $e^{i[\varphi_\sigma(t)+\omega_r t]}$ on the axis in the complex plane defined by the unit vector $e^{-i\Delta t}$. In order to determine the phase uniquely, the projection on at least two different axes should be known. Therefore, at least two measurements at two different velocities should be performed. Together with the two intensity measurements of $|\vec{E}_r(t)|^2$ and $|\vec{E}_s(t)|^2$, this brings the minimum number of measurements to four.

Note that the most accurate phase determination can be established if the Doppler shifts $\Delta_1$ and $\Delta_2$ are chosen such that the axes defined by $e^{-i\Delta_1 t}$ and $e^{-i\Delta_2 t}$ are orthogonal. However, since these axes are rotating in time, the most convenient velocities are also time dependent. Therefore, it is favorable to operate the velocity drive in a continuous mode and to register for each delayed photon both its time delay and the velocity of the reference sample. This has the additional advantage that there is an intrinsic normalization of the data for each time and velocity channel.

For a certain time delay $t_0$, the phase difference[22] $\varphi_\sigma(t_0) + \omega_r t_0$ can be determined from a three-parameter fit of the velocity spectrum $I(t_0, \Delta)$. The parameters are the baseline, $|\vec{E}_r(t_0)|^2 + |\vec{E}_s(t_0)|^2$, the amplitude of the cosine function, $2|E_\sigma(t_0)||E_r(t_0)|$, and the phase difference. Note that $|E_r(t_0)|$ is proportional to the square root of the delayed intensity after the reference sample alone. Hence, together with the amplitude of the cosine function, $2|E_\sigma(t_0)||E_r(t_0)|$, the magnitude of the $\sigma$ component of the unknown wave field, $|E_\sigma(t_0)|$, can be determined. Consequently, the presented scheme allows for the full determination of the $\sigma$ component of the wave field. Since the reference wave field has no $\pi$ component, an experiment with a single-line reference sample cannot provide information on the $\pi$ component of the investigated wave field. However, this information could be accessed by using an optically active reference sample.

In order to demonstrate the experimental feasibility of the concept, experiments were carried out at the Advanced Photon Source, Argonne, Illinois. The beam energy was tuned to the 14.413 keV resonance energy in $^{57}$Fe. A 95% $^{57}$Fe enriched stainless steel foil (SS310) of 0.93 $\mu$m thickness

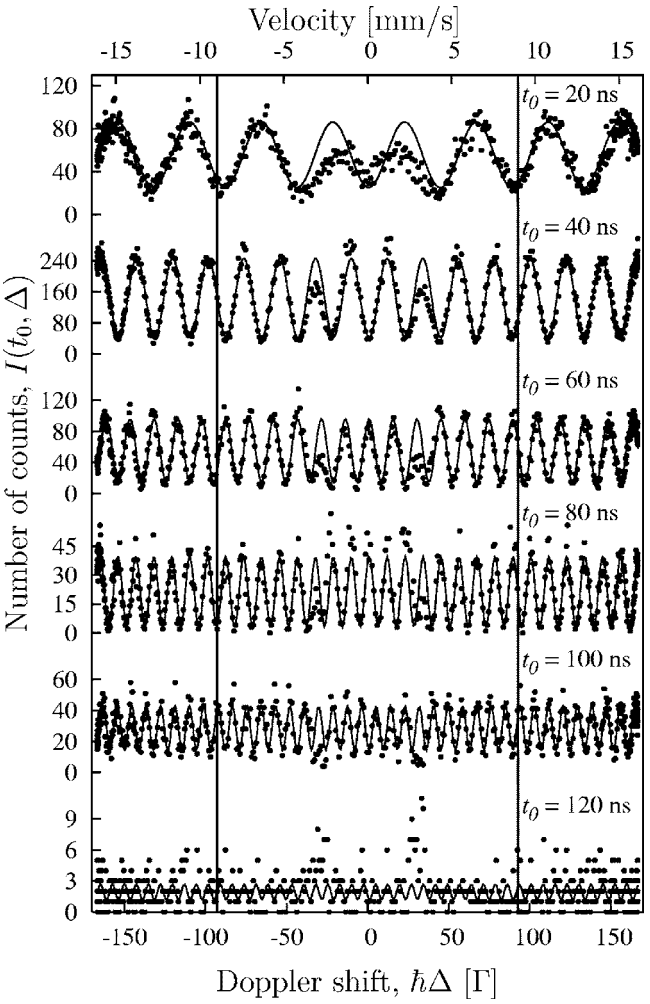


FIG. 2. Experimental data for a natural $\alpha$-iron foil of 50 $\mu$m thickness with the hyperfine field aligned perpendicular to the propagation and polarization direction of the incident radiation. The solid lines are fits excluding the region from −9 to 9 mm/s.

served as reference sample. In order to reduce the errors on the velocity, the velocity drive was operated in a sinusoidal mode. The sinusoidal mode also has the advantage that the measuring time at high velocities (the region of interest) is longer than at low velocities. The investigated sample was a natural $\alpha$-iron foil of 50 $\mu$m thickness, which was magnetized in three different directions in the plane perpendicular to the propagation direction of the radiation using a small external field.

In the first experiment, the external field was applied perpendicular to the polarization direction of the incident radiation. For this geometry, only two transitions can be excited and no optical activity is observed. The velocity spectra for various time channels are shown in Fig. 2. The width of one time channel is 0.246 ns, thus the time integration is mainly determined by the detector resolution of 1.1 ns. A sinusoidal behavior with a frequency depending on the time delay can be observed. For the analysis, the velocity region between −9 and 9 mm/s was excluded.[23] This was done because a strong radiative coupling distorting the cosine function was expected near ±3 mm/s. The remaining regions were fitted with the three parameters mentioned above. Since for certain channels the number of counts is quite low, we performed the analysis according to the maximum likelihood estimation applied to Poisson distributed data.[24]

The results of this analysis are shown on the left-hand side of Fig. 3. The upper panel displays the norm, the phase difference with the reference field, the real part, and the imaginary part of the $\sigma$ component of the nuclear resonantly scattered wave field as a function of time. The solid line is a fit of the time spectra using the software package CONUSS.[25,26] The fitted values are 32.61(2) T for the magnetic field and 0.094(4) mm/s for the isomer shift. The norm of the wave field shows a typical quantum beat behavior. For the difference in phase between the investigated and the reference wave field an overall linear variation is observed, with a slope depending on the isomer shift. Moreover, phase jumps of $\pi$ occur at those time delays for which the wave field vanishes. Note that although there is a discontinuity in the phase, the wave field itself is a continuous time function. This is clear from the time evolution of the real and the imaginary part of the wave field.

Figure 3 also shows the results for the hyperfine field oriented at 0° and 30° with respect to the polarization direction. The data of the central panel were obtained after only 15 min of data acquisition. Comparison with the other data shows that extending the acquisition time mainly affects the accuracy at late times where the count rate is low. For the 30° orientation the sample is optically active, which means that the nuclear resonantly scattered radiation has both a $\sigma$ and a $\pi$ component. However, since we used a single-line reference sample, we were only sensitive to the $\sigma$ component.

An important application of phase determination is the transformation to reciprocal space. The energy dependence of the $\sigma$ component of the wave field can be found by a Fourier transformation. Note that for this transformation only a finite time window is available, giving rise to truncation

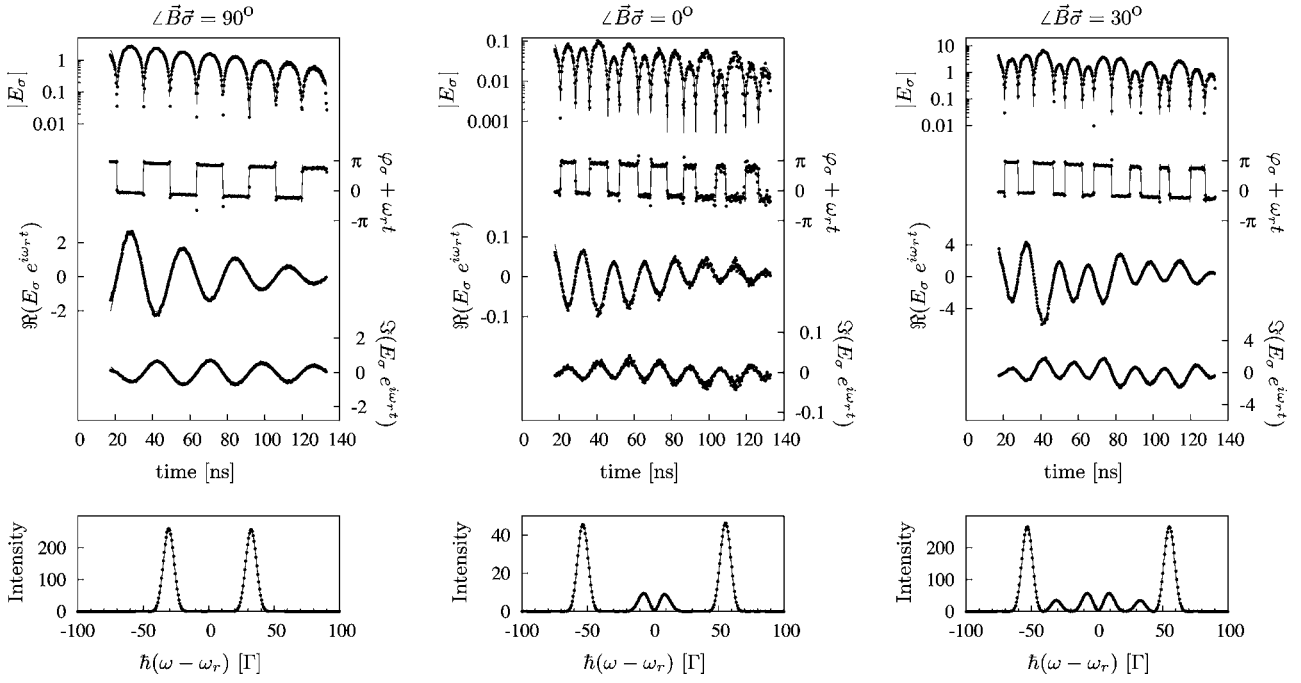


FIG. 3. $\sigma$ component of the wave field after nuclear resonant scattering by a natural $\alpha$-iron foil of 50 $\mu$m thickness with the hyperfine field aligned along different directions in the plane perpendicular to the propagation direction of the incident radiation. Left: The hyperfine field perpendicular to the polarization direction (acquisition time: 8.3 h at an average delayed count rate of 410 Hz). Center: The hyperfine field parallel to the polarization direction (acquisition time: 15 minutes at an average delayed count rate of 470 Hz). Right: The hyperfine field at 30° with respect to the polarization direction (acquisition time: 16 h at an average delayed count rate of 525 Hz). Top: The time evolution of the norm, the phase difference with the reference field, the real, and the imaginary part. Bottom: The reconstructed energy spectrum. The dots are obtained from the experimental data, the solid line is a fit using the code CONUSS.

wiggles. The wiggles can be reduced by smoothing the time window, which is, however, at the expense of the energy resolution. For the energy reconstruction shown in the lower panels of Fig. 3, a square window lasting from 17 till 133 ns was multiplied by a Gaussian with a full width at half maximum of 68 ns. The energy scale is given in units of the natural linewidth of the Mössbauer level in $^{57}$Fe, $\Gamma = 4.66$ neV. One can clearly observe two, four, and six allowed transitions. Another possible application of phase determination in nuclear resonant scattering experiments is the structure determination of complex systems, e.g., biomolecules. Similar to the approach using a radioactive source,[27,28] measurements in and out of resonance for different scattering angles should then be combined.

In conclusion, a simple experimental scheme for phase determination in nuclear resonant scattering experiments was developed and demonstrated for the case of nuclear forward scattering by an $\alpha$-iron foil. It was shown that the results can be used to construct energy spectra. A great advantage of the proposed scheme is that the experimental setup is easy to realize, which opens perspectives towards various applications using more complicated scattering geometries or sample environments.

The authors would like to thank R. Coussement for the many fruitful discussions. This work was supported by the Fund for Scientific Research-Flanders (G.0224.02 and G.0498.04), the Inter-University Attraction Pole (IUAP P5/1), and the Concerted Action of the KULeuven (GOA/2004/02). Use of the Advanced Photon Source was supported by the U.S. DOE, Office of Science, under Contract No. W-31-109-Eng-38. R. Callens, C. L'abbé, and J. Meersschaut thank the FWO-Flanders for financial support.

[1] D. Gabor, Nature (London) **161**, 777 (1948).
[2] E. Gerdau, R. Rüffer, H. Winkler, W. Tolksdorf, C. P. Klages, and J. P. Hannon, Phys. Rev. Lett. **54**, 835 (1985).
[3] Hyperfine Interact. **123/124** (1999); Hyperfine Interact. **125** (2000), special issues on nuclear resonant scattering of synchrotron radiation, edited by E. Gerdau and H. de Waard.
[4] R. Röhlsberger, *Nuclear Condensed Matter Physics with Synchrotron Radiation* (Springer, Berlin, 2004).
[5] S. Nasu, Hyperfine Interact. **113**, 97 (1998).
[6] G. Wortmann, K. Rupprecht, and H. Giefers, Hyperfine Interact.. **144/145**, 103 (2002).
[7] W. L. Mao, W. Sturhahn, D. L. Heinz, H. K. Mao, J. F. Shu, and R. J. Hemley, Geophys. Res. Lett. **31**, L15618 (2004).
[8] L. Niesen, A. Mugarza, M. F. Rosu, R. Coehoorn, R. M. Jungblut, F. Roozeboom, A. Q. R. Baron, A. I. Chumakov, and R. Rüffer, Phys. Rev. B **58**, 8590 (1998).
[9] D. L. Nagy, L. Bottyan, B. Croonenborghs, L. Deak, B. Degroote, J. Dekoster, H. J. Lauter, V. Lauter-Pasyuk, O. Leupold, M. Major, J. Meersschaut, O. Nikonov, A. Petrenko, R. Rüffer, H. Spiering, and E. Szilagyi, Phys. Rev. Lett. **88**, 157202 (2002).
[10] R. Röhlsberger, T. Klein, K. Schlage, O. Leupold, and R. Rüffer, Phys. Rev. B **69**, 235412 (2004).
[11] C. L'abbé, J. Meersschaut, W. Sturhahn, J. S. Jiang, T. S. Toellner, E. E. Alp, and S. D. Bader, Phys. Rev. Lett. **93**, 037201 (2004).
[12] R. Röhlsberger, J. Bansmann, V. Senz, K. L. Jonas, A. Bettac, O. Leupold, R. Rüffer, E. Burkel, and K. H. Meiwes-Broer, Phys. Rev. Lett. **86**, 5597 (2001).
[13] R. Röhlsberger, J. Bansmann, V. Senz, K. L. Jonas, A. Bettac, K. H. Meiwes-Broer, and O. Leupold, Phys. Rev. B **67**, 245412 (2003).
[14] Y. Hasegawa, Y. Yoda, K. Izumi, T. Ishikawa, S. Kikuta, X. W. Zhang, and M. Ando, Phys. Rev. B **50**, R17748 (1994).
[15] W. Sturhahn, C. L'abbé, and T. S. Toellner, Europhys. Lett. **66**, 506 (2004).
[16] A. Q. R. Baron, H. Franz, A. Meyer, R. Rüffer, A. I. Chumakov, E. Burkel, and W. Petry, Phys. Rev. Lett. **79**, 2823 (1997).
[17] G. V. Smirnov, V. G. Kohn, and W. Petry, Phys. Rev. B **63**, 144303 (2001).
[18] W. Potzel, U. van Bürck, P. Schindelmann, G. M. Kalvius, G. V. Smirnov, E. Gerdau, Y. Shvyd'ko, H. D. Rüter, and O. Leupold, Phys. Rev. A **63**, 043810 (2001).
[19] R. Callens, R. Coussement, T. Kawakami, J. Ladrière, S. Nasu, T. Ono, I. Serdons, K. Vyvey, T. Yamada, Y. Yoda, and J. Odeurs, Phys. Rev. B **67**, 104423 (2003).
[20] W. Sturhahn, Phys. Rev. B **63**, 094105 (2001).
[21] The contribution of electronic scattering can be described by a scaling factor. Since this factor is the same for both scattering paths, it can be omitted without loss of generality.
[22] The phase difference $\varphi_\sigma(t_0)+\omega_r t_0$ is the difference in phase due to the nuclear resonant scattering process; this technique is not sensitive to the phase change due to electronic scattering.
[23] Thirty-seven percent of the data is located in this excluded region.
[24] T. Hauschild and M. Jentschel, Nucl. Instrum. Methods Phys. Res. A **457**, 384 (2001).
[25] W. Sturhahn and E. Gerdau, Phys. Rev. B **49**, 9285 (1994).
[26] W. Sturhahn, Hyperfine Interact. **125**, 149 (2000).
[27] P. J. Black, Nature (London) **206**, 1223 (1965).
[28] F. Parak, R. L. Mössbauer, and U. Biebl, Z. Phys. **244**, 456 (1971).